

Third-harmonic-generation study of orientational order in nematic liquid crystals

K. Y. Wong and A. F. Garito

*Department of Physics, University of Pennsylvania, Philadelphia, Pennsylvania 19104-6396
and Laboratory for Research on the Structure of Matter, University of Pennsylvania, Philadelphia, Pennsylvania 19104-3859
(Received 7 July 1986)*

Relationships between the optical third-harmonic-generation susceptibility $\chi_{ijkl}^{(3)}(-3\omega; \omega, \omega, \omega)$ and the nonvanishing order parameters $\langle P_2 \rangle$ and $\langle P_4 \rangle$ for a nematic-liquid-crystal phase are presented. Third-harmonic-generation experiments were performed on the nematic *N*-(*p*-methoxybenzylidene)-*p*-butylaniline (MBBA) using the wedge-maker fringe method as a function of polarization and temperature to demonstrate the simultaneous determination of $\langle P_2 \rangle$ and $\langle P_4 \rangle$. The results are in agreement with previous experimental results from nuclear magnetic resonance and Raman scattering studies. Local-field corrections are considered, and based on the data, local-field factors do not appear to depend on the long-range anisotropy of the macroscopic medium.

I. INTRODUCTION

Considerable progress has been achieved in understanding the nature of orientational order in liquid-crystal phases.¹ For the simplest case of a nematic phase, orientational ordering has been measured for the two nonvanishing lowest-order parameters $\langle P_2 \rangle$ and $\langle P_4 \rangle$. Whereas the relationships between $\langle P_2 \rangle$ and a variety of experimental spectroscopic quantities have been consistently established, only a few important ones have been examined for $\langle P_4 \rangle$, notably Raman scattering,² two-photon absorption,³ and dc-induced second-harmonic generation.⁴ At the same time, continuing studies of the nonlinear optical properties of π -electron conjugated organic and polymer structures have demonstrated large nonlinear electronic susceptibilities for a large number of structures, phases, and states, including mesogenic structures and liquid-crystal phases.^{5,6} Such large higher-order electronic responses potentially allow independent determinations of $\langle P_2 \rangle$ and $\langle P_4 \rangle$ by a variety of nonlinear optical process. In this paper, we examine relationships between orientational order and optical third-harmonic generation. Analytic expressions are derived that allow the simultaneous determination of the order parameters $\langle P_2 \rangle$ and $\langle P_4 \rangle$ based on optical third-harmonic-generation studies. Local-field corrections are considered, and several conclusions are drawn based on experimental measurements.

The nematic-liquid-crystal phase displays long-range orientational order while possessing short-range positional order.¹ The constituent molecules usually have an elongated planar structure consisting of a rigid central "backbone" and a somewhat flexible hydrocarbon "tail." The bulk nematic phase, however, is uniaxial and has an infinite rotational symmetry along this axis. The director \hat{n} is defined as the unit vector along this axis of symmetry. The absence of piezoelectricity in this phase demonstrates that \hat{n} and $-\hat{n}$ are equivalent. If we assume the molecule to be strictly rigid, the long-range orientational order can be described by an orientational distribution function $F(\phi, \theta, \psi)$ (Ref. 2), which is the probability that a molecule has an orientation with Euler angles (ϕ, θ, ψ)

with respect to the laboratory frame (x, y, z) , where the z axis is defined to be parallel to the director \hat{n} . The assumed rigidity of the molecules is often justified by the fact that it is the central rigid backbone that contributes almost all of the magnetic and dielectric anisotropy.⁷⁻⁹ A similar argument also applies in the case of nonlinear optics, since the π -electron system of the central aromatic rings possess unusually large nonlinear optical susceptibilities.^{5,6,10}

The orientational distribution function can be simplified by imposing the symmetry of the macroscopic liquid-crystal phase. For a uniaxial macroscopic phase with the unique axis parallel to the z axis, the orientational distribution function is independent of ϕ . A commonly adopted simplification is to assume the molecule to be cylindrically symmetric along its long axis.² Under this assumption, $F(\phi, \theta, \psi)$ is independent of ψ , and we are left with a single variable function $F(\theta)$. $F(\theta)$ can be expanded in terms of Legendre polynomials

$$F(\theta) = \sum_{l=0}^{\infty} \frac{2l+1}{2} A_l P_l(\cos\theta) \quad (1)$$

with

$$A_l = \int_0^{\pi} d\theta \sin\theta [F(\theta) P_l(\cos\theta)] \equiv \langle P_l \rangle. \quad (2)$$

The equivalence of \hat{n} and $-\hat{n}$ in a nematic phase implies that only $\langle P_l \rangle$ with l even are nonzero. Since $\langle P_0 \rangle$ is related only to the normalization of the distribution function, the lowest-order nonvanishing order parameters are thus $\langle P_2 \rangle$ and $\langle P_4 \rangle$.

This paper is arranged as follows. In Sec. II we derive relations between the third-order macroscopic susceptibility and the microscopic molecular susceptibility in the nematic phase, and show that measurements of third-harmonic generation with different polarization can lead to a determination of $\langle P_2 \rangle$ and $\langle P_4 \rangle$. The experimental design for measurements of the polarization and temperature dependence of the third-harmonic susceptibility is described in Sec. III. In Sec. IV the results are presented and discussed with conclusions drawn.

II. THIRD-HARMONIC GENERATION IN A NEMATIC LIQUID CRYSTAL

Optical third-harmonic generation in a medium is described by the macroscopic third-order susceptibility tensor $\chi_{ijkl}^{(3)}(-3\omega; \omega, \omega, \omega)$ which can be related to the corresponding microscopic molecular susceptibility $\gamma_{ijkl}(-3\omega; \omega, \omega, \omega)$ through orientational averaging. In general, the orientational average of an l th rank tensor involves up to the l th order of the statistical average of the Legendre polynomial $\langle P_l \rangle$. Thus the study of third-harmonic generation in a nematic-liquid-crystal phase can reveal information about $\langle P_2 \rangle$ and $\langle P_4 \rangle$. The polarization at the third-harmonic frequency $P^{3\omega}$ produced by an applied optical field E at frequency ω is given by

$$P_i^{3\omega} = \chi_{ijkl}^{(3)} E_j^\omega E_k^\omega E_l^\omega. \quad (3)$$

The polarization $P^{3\omega}$ originates from the microscopic third-harmonic polarization $p^{3\omega}$ of individual molecules driven by the local field E_{loc}^ω , with $p^{3\omega}$ given by

$$p_{i'}^{3\omega} = \gamma_{i'j'k'l'}(E_{loc}^\omega)_{j'}(E_{loc}^\omega)_{k'}(E_{loc}^\omega)_{l'}, \quad (4)$$

where the primed coordinate designates the molecular fixed axes, with the z' axis along the molecular long axis. The local field can be related to the macroscopic field by the local-field correction tensor f_s^ω , which, in general, depends on the properties and orientation of the molecule at which the local field is considered

$$(E_{s,loc}^\omega)_{i'} = (f_s^\omega)_{i'j'} E_{j'}^\omega. \quad (5)$$

In the Lorentz-Lorentz model for an isotropic liquid, f^ω is a scalar given by

$$f^\omega = \frac{2 + (n^\omega)^2}{3}, \quad (6)$$

where n^ω is the refractive index at frequency ω . The macroscopic polarization $P^{3\omega}$ is a sum over microscopic polarization, taking account of the local field at frequency 3ω

$$P_i^{3\omega} = \sum_{s=1}^N R_{ii'}^S (f_s^{3\omega})_{i'j'} (p_s^{3\omega})_{j'}, \quad (7)$$

where the summation is over all N molecules within a unit volume. R^S is the rotation matrix transforming the molecular frame to the laboratory frame.

With Eqs. (3), (4), (5), and (7), we can relate the macroscopic $\chi_{ijkl}^{(3)}$ to the microscopic $\gamma_{i'j'k'l'}$ and obtain

$$\chi_{ijkl}^{(3)} = N \langle R_{im'} R_{jn'} R_{k'o'} R_{lp'} f_{m'i'}^{3\omega} \gamma_{i'j'k'l'} f_{j'n}^\omega f_{k'o}^\omega f_{l'p'}^\omega \rangle, \quad (8)$$

where $\langle \rangle$ represents an average over the orientational distribution. The local-field correction tensor f in general involves a complicated expression for anisotropic media.¹¹ We will rely instead on experimental information to simplify the evaluation of Eq. (8). For the case of the linear polarizability, α , it has been experimentally demonstrated that at all temperatures in the nematic-liquid-crystal phase, the following expression holds:¹²

$$\langle \alpha \cdot f \rangle_{||} - \langle \alpha \cdot f \rangle_{\perp} \propto \langle \alpha \rangle_{||} - \langle \alpha \rangle_{\perp}, \quad (9)$$

where $||$ and \perp correspond to the components parallel and perpendicular to the nematic director, respectively. For the proportionality in Eq. (9) to hold for all temperatures, the local-field correction tensor f must be independent of the long-range anisotropy of the bulk. It has been suggested¹² that the local-field correction tensor f should be diagonalized in the same principal axes as α , and is thus molecule fixed. The interaction between molecules which give rise to the local-field correction are short-range dipole-dipole mediated. The local-field correction at a molecule would then have contributions predominantly from its nearest neighbors, and thus should be insensitive to the long-range anisotropy of the medium. Furthermore, these nearest neighbor correlations are not significantly temperature dependent and probably do not change even through the nematic to isotropic phase transition.

Assuming that the local-field correction tensor is molecule fixed, we can extend this idea to our discussion in nonlinear optics and define a "dressed" molecular susceptibility γ^* , which has the same principle axes as the "bare" susceptibility γ , by

$$\gamma_{i'j'k'l'}^* = f_{i'i'}^{3\omega} f_{j'j'}^\omega f_{k'k'}^\omega f_{l'l'}^\omega \gamma_{i'j'k'l'} \quad (\text{no summation implied}) \quad (10)$$

so that Eq. (8) assumes a more simple form

$$\chi_{ijkl}^{(3)} = N \langle R_{ii'} R_{jj'} R_{kk'} R_{ll'} \gamma_{i'j'k'l'}^* \rangle. \quad (11)$$

The measurement of the third-harmonic susceptibility is performed on those components along the principal axis of the bulk phase. We are thus interested in the dependence of the macroscopic tensors $\chi_{zzz}^{(3)}$ and $\chi_{xxxx}^{(3)}$ on the microscopic tensor $\gamma_{i'j'k'l'}$. Here z is chosen to be along the nematic director. The evaluation of Eq. (11) for these two tensors is given in the Appendix. The results are

$$\chi_{zzz}^{(3)} = N(\delta + 2\xi \langle P_2 \rangle + 8\eta \langle P_4 \rangle), \quad (12a)$$

$$\chi_{xxxx}^{(3)} = N(\delta - \xi \langle P_2 \rangle + 3\eta \langle P_4 \rangle), \quad (12b)$$

$$\chi_{iso}^{(3)} = N\delta. \quad (12c)$$

The dependence of the parameters δ , ξ , and η on the dressed molecular susceptibilities is given in Eqs. (A4)–(A6) of the Appendix. $\chi_{iso}^{(3)}$ is the susceptibility for the isotropic phase where $\langle P_2 \rangle$ and $\langle P_4 \rangle$ vanish. We assume that the change in density as a function of temperature and over the phase transition is negligible. We see from Eq. (12) that the third-order susceptibilities $\chi_{zzz}^{(3)}$ and $\chi_{xxxx}^{(3)}$ are functions of temperature in the nematic phase as a result of the temperature dependence of $\langle P_2 \rangle$ and $\langle P_4 \rangle$. They become temperature independent after the phase transition to the isotropic phase.

The order parameters $\langle P_2 \rangle$ and $\langle P_4 \rangle$ could be determined from the experimental results of $\chi_{zzz}^{(3)}$, $\chi_{xxxx}^{(3)}$, and $\chi_{iso}^{(3)}$ if the parameters δ , ξ , and η are known. The bare molecular susceptibility γ_{ijkl} could in principle be calculated by perturbation theory using a scheme similar to that developed by Lalama and Garito^{5,6,10} for the second-order susceptibility. However, since the parameters δ , ξ , and η are dependent on the dressed susceptibility instead, to calculate these parameters would require that the local-field correction factor be known *a priori*. Thus, it

would appear that Eqs. (12) are not sufficient for the calculation of the order parameter due to the lack of information regarding the local-field correction.

For rodlike molecules such as those comprising the nematic phase, the third-order susceptibility has its largest component along the long molecular axis due to the delocalization of π electrons along the conjugated central backbone.^{5,6,10} To a first approximation, we can then assume $\chi_{zzz}^{(3)}$ to be the only nonvanishing component. From Eq. (12) we have

$$\frac{\chi_{zzz}^{(3)} + 2\chi_{xxxx}^{(3)}}{\chi_{iso}^{(3)}} = 3 + K_4 \langle P_4 \rangle, \quad (13)$$

where $K_4 = 14(\eta/\delta)$. If we assume that only $\chi_{zzz}^{(3)}$ is nonzero, we obtain $K_4 = 2$ from Eqs. (A4)–(A6). We notice that the constant K_4 is not very sensitive to the inclusion to a reasonable magnitude of the other components of γ_{ijkl} . For example, if we assume the second contributing component of the molecular susceptibility to be χ_{xxxx} , we get $K_4 = 1.75$ for $\chi_{xxxx} = 0.25\chi_{zzz}^{(3)}$. This would amount to a 12% difference in the determination of the value of $\langle P_4 \rangle$, which is much smaller than the uncertainty of the reported value of $\langle P_4 \rangle$ determined by the Raman scattering method.²

Similarly, from Eq. (12) we have

$$\frac{3\chi_{zzz}^{(3)} - 8\chi_{xxxx}^{(3)}}{\chi_{iso}^{(3)}} = K_2 \langle P_2 \rangle - 5, \quad (14)$$

where $K_2 = 14(\xi/\delta)$. The magnitude and temperature dependence of $\langle P_2 \rangle$ have been measured previously with very good precision. Using the reported values of $\langle P_2 \rangle$ together with the experimentally determined values of $\chi_{zzz}^{(3)}$, $\chi_{xxxx}^{(3)}$, and $\chi_{iso}^{(3)}$ we can fix the parameter K_2 . The parameter K_2 , however, depends only upon the relative magnitudes of the molecular susceptibilities and should not have any temperature dependence. Thus, if we fix the parameter K_2 at one temperature, then based on the value of K_2 , the values of $\langle P_2 \rangle$ at other temperatures can be determined experimentally. Comparison of the values of $\langle P_2 \rangle$ obtained in this way with the reported values of $\langle P_2 \rangle$ should provide a test of the overall reliability of the experimental data. Furthermore, it would also provide more information for the estimation of parameter K_4 and thus for the determination of $\langle P_4 \rangle$.

III. EXPERIMENTS

Measurements of the temperature dependence of the third-harmonic susceptibility parallel and perpendicular to the nematic director $\chi_{zzz}^{(3)}$ and $\chi_{xxxx}^{(3)}$ in the nematic phase and $\chi_{iso}^{(3)}$ in the isotropic phase were performed. The experimental design was based on the wedged maker fringe method.¹³ The liquid-crystal sample was formed into a wedged shape to allow variation of the sample thickness. The third harmonic generated from the sample was measured as a function of the sample thickness. The third-harmonic susceptibility is determined by calibrating with the result obtained from an identical experiment performed on a material with known third-harmonic susceptibility.

The optical design for the third-harmonic-generation experiment is shown in Fig. 1. A Q -switched Nd:YAG (where YAG represents yttrium aluminum garnet) laser (Quanta Ray) was used as a pump beam into a compressed hydrogen gas cell, generating a first Stokes line from stimulated Raman scattering with wavelength $\lambda = 1.91 \mu\text{m}$. The Stokes line, after separation from the pump beam using a dispersive prism, was split into a reference beam and a pump beam. The reference beam passed through a BK-7 glass plate R to provide a reference third-harmonic signal that was detected by the photomultiplier tube PMT1. The purpose of the reference was to account for the effects due to laser-power fluctuations. The sample beam acted as the input beam for third-harmonic generation in the liquid-crystal sample S .

The liquid-crystal sample was contained between two surface-treated glass plates spaced by a glass fiber, forming a wedged shape. The glass plate was coated with polyvinylalcohol (PVA) followed by a unidirectional rubbing for the desired uniaxial homogeneous alignment.¹⁴ The liquid crystal N -(p -methoxybenzylidene)- p -butylaniline (MBBA) (Aldrich Chemical Company, Inc.) was chosen as the material for investigation so that direct comparison could be made with the Raman scattering results.^{2,15} The wedge shape sample had thickness varying from $\sim 0 \mu\text{m}$ to $50 \mu\text{m}$. The sample was mounted on a temperature stabilized heating cell which was in turn mounted inside a vacuum chamber.^{16,17} The sample assembly was positioned on a stepper motor driven translation stage, so that translation across the laser beam resulted in the variation of the sample thickness. The sample third-harmonic signal was detected by PMT2. The ratio of the two outputs from PMT1 and PMT2 was independent of the input beam power, and therefore effects caused by fluctuations in beam power were minimized. Control of data acquisition and signal averaging were performed through an interface to a PDP 11/23 microcomputer.

The intensity of the generated third-harmonic signal from the sample in our configuration can be derived to obtain

$$I_{3\omega}(l) = A (48\pi/c^2)^2 \omega^2 (\chi^{(3)})^2 I_c^2 I_\omega^3 \sin^2(\pi l/2l_c), \quad (15)$$

where

$$A = \left[\frac{2}{1+n_G^\omega} \right]^6 \left[\frac{2n_G^\omega}{n_S^\omega + n_G^\omega} \right]^6 \left[\frac{2n_G^{3\omega}}{1+n_G^{3\omega}} \right]^2 \left[\frac{1}{n_S^{3\omega} + n_G^{3\omega}} \right]^2 \\ \times \left[\frac{2n_S^{3\omega}}{n_S^{3\omega} + n_G^{3\omega}} \right] \left[\frac{n_S^\omega + n_S^{3\omega}}{n_S^{3\omega} + n_G^{3\omega}} \right] \left[\frac{n_S^\omega + n_G^{3\omega}}{n_S^{3\omega} + n_G^{3\omega}} \right]. \quad (16)$$

The subscripts S and G label the refractive indices corresponding to the liquid crystal and glass, respectively. I_ω is the fundamental beam intensity, l is the sample thickness, and l_c is the coherence length of the liquid-crystal sample given by

$$l_c = \frac{\lambda}{6(n^{3\omega} - n^\omega)}. \quad (17)$$

The third-harmonic generation from the glass plate was shown to be negligible in this case.

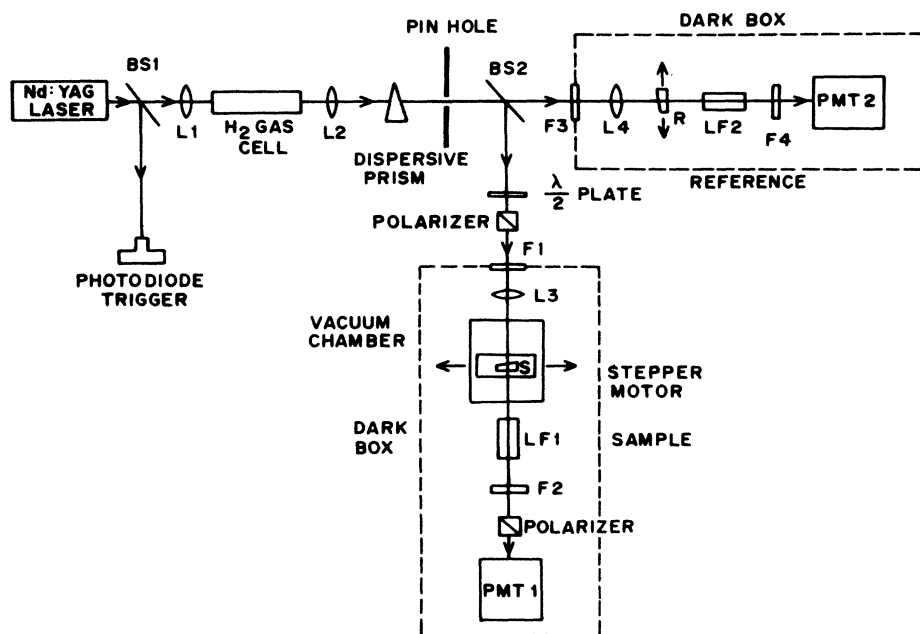


FIG. 1. Optical design for the third-harmonic-generation experiment. L1–L4, focusing lenses; BS1 and BS2, beam splitters; F1–F4, LF1, and LF2, optical filters; R, reference BK-7 glass wedge; S, liquid-crystal sample; PMT1 and PMT2, photomultiplier tubes.

The average input power levels were approximately 0.5 mJ per pulse of 10 ns duration, focused to a spot of approximately 10^{-3} cm². The third-harmonic power generated from a fixed spot in the sample was continuously monitored for a few minutes with no significant change of power level observed, showing that the effects of heating and optical field induced director reorientation were negligible. The maker interference patterns were obtained by recording the third-harmonic power as the sample was translating across the beam. Typical output fringes are shown in Fig. 2, where adjacent data points are connected by straight lines. A measurement typically spanned a translation distance of 1 cm over the sample. The sample uniformity is clearly reflected in the quality of the fringes. The uniform height of the maker fringe peaks also shows

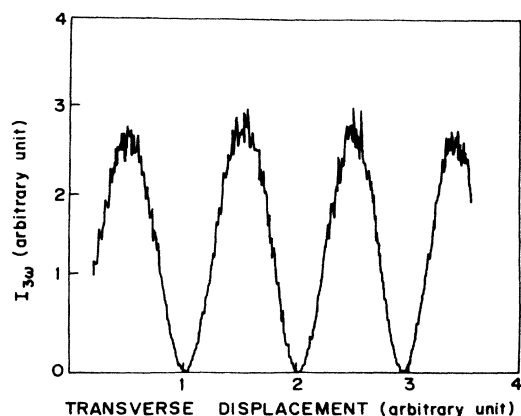


FIG. 2. Typical output fringes in the third-harmonic-generation measurements of MBBA.

that there is no thickness dependence of $\chi^{(3)}$, and thus of $\langle P_2 \rangle$ and $\langle P_4 \rangle$ in the sample. The maker fringe data are analyzed using a least-squares procedure for the fitting function

$$y = A_1 \sin^2 \left[\frac{\pi l}{2A_3} + \frac{A_4}{2} \right] + A_2, \quad (18)$$

where $(A_1 + A_2)$ and A_2 are, respectively, the maximum and minimum of each measured fringe, A_3 is the coherence length l_c of the sample, and A_4 is the phase offset. The measurement was repeated with a BK-7 glass wedge in place of the sample, which allowed the $\chi^{(3)}$ of the liquid-crystal sample to be determined relative to the reported value of 4.67×10^{-14} esu for the BK-7 glass.¹⁸

Measurements of $\chi^{(3)}$ were performed on the two principal components $\chi_{zzz}^{(3)}$ and $\chi_{xxxx}^{(3)}$ in the nematic phase for different temperatures. For an input beam polarized along the z axis (x axis), the symmetry of the bulk nematic phase implies that the output third-harmonic beam should be linearly polarized along the z axis (x axis) and coupled only to the $\chi_{zzz}^{(3)}$ ($\chi_{xxxx}^{(3)}$) component of the susceptibility. Deviation of the input beam polarization from the principal axis would result in a rotated elliptical polarization of the output third-harmonic beam. By monitoring the polarization properties of the output beam, the input polarization was adjusted to ensure best coincidence with the principal axis of the liquid-crystal sample. The susceptibility $\chi_{iso}^{(3)}$ in the isotropic phase was also measured for different temperatures. The input polarization independence of $\chi_{iso}^{(3)}$ was established, which ensures that there was no instrumental anisotropy. Measurements were performed on four different samples, and, within experimental error, there was no sample dependence.

IV. RESULTS AND DISCUSSION

The results of the measurement of the third-order nonlinear susceptibility $\chi^{(3)}$ for the MBBA in the nematic phase and in the isotropic phase are given in Fig. 3. Before we proceed to calculate the order parameters $\langle P_2 \rangle$ and $\langle P_4 \rangle$, we will first examine the results for the coherence length which are given in Fig. 4. Since the coherence length is related only to the linear refractive index, which has been studied previously,^{12,19} this could serve as a consistency check of our data. Earlier studies¹² show that the quantity \bar{n}^2/ρ [where $\bar{n}^2 = (n_{||}^2 + 2n_{\perp}^2)/3$, $n_{||}$ and n_{\perp} are the refractive indices parallel and perpendicular to the nematic director, respectively, and ρ is the density of the liquid crystal] is temperature independent throughout the nematic and isotropic phases. With this assumption and using Eq. (17), we can derive a relation between the coherence lengths $l_{||}$, l_{\perp} , and l_{iso} , $l_{||}$ and l_{\perp} are the coherence lengths measured parallel and perpendicular to the director in the nematic phase, respectively, and l_{iso} is the coherence length measured in the isotropic phase. We get

$$\frac{1}{l_{iso}} = \frac{1}{3} \left[\frac{1}{l_{||}} \frac{n_{||}^{3\omega} + n_{||}^{\omega}}{n_{iso}^{3\omega} + n_{iso}^{\omega}} + \frac{2}{l_{\perp}} \frac{n_{\perp}^{3\omega} + n_{\perp}^{\omega}}{n_{iso}^{3\omega} + n_{iso}^{\omega}} \right], \quad (19)$$

where we consider negligible the small variation of ρ with temperature. Using the experimental values for $l_{||}$ and l_{\perp} at different temperatures, we have calculated the expected values for l_{iso} . The results are also shown in Fig. 4. We see that the predicted values of l_{iso} calculated from $l_{||}$ and l_{\perp} at different temperatures in the nematic phase closely correspond to the actual value of l_{iso} measured in the isotropic phase. The slight discrepancy is probably due to the small variation of the density with temperature which we have neglected. In fact, the predicted values of l_{iso} fit very well on a straight line with the measured value of l_{iso} in the isotropic phase with no apparent discontinuity at the phase transition temperature. Our data thus show very good agreement with previous studies of the linear refractive index in the liquid-crystal phase.

The order parameter $\langle P_2 \rangle$ is calculated from the exper-

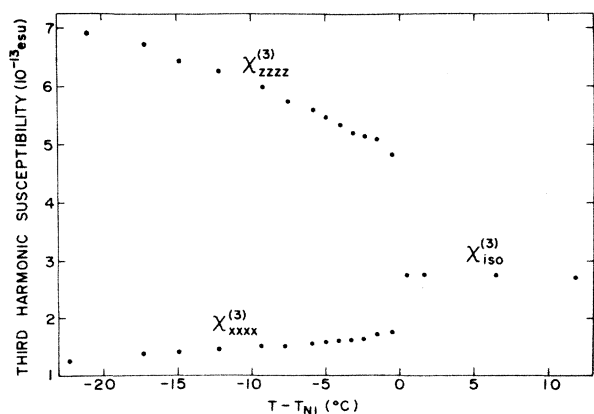


FIG. 3. Measured third-harmonic susceptibility of MBBA as function of temperature; z axis and x axis are parallel and perpendicular to the director, respectively.

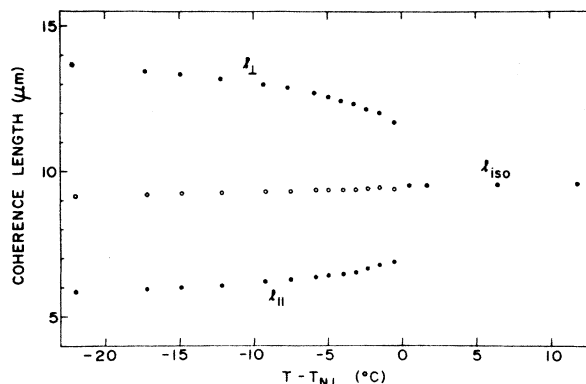


FIG. 4. Coherence length of MBBA as function of temperature. ●, experimental results for the coherence length parallel ($l_{||}$), perpendicular (l_{\perp}) to the director and in the isotropic phase (l_{iso}); ○, predicted value of l_{iso} calculated from Eq. (19).

imental results of the third-order susceptibility using Eq. (14). We determined the parameter K_2 in Eq. (14) by the reported value of $\langle P_2 \rangle$ at one temperature, and deduce independently the values of $\langle P_2 \rangle$ at other temperatures. From NMR results,²⁰ the value of $\langle P_2 \rangle$ at $T - T_{NI} = -21^\circ\text{C}$ is 0.6. Using this value of $\langle P_2 \rangle$ with our results, we get $K_2 = 14.7$. The values of $\langle P_2 \rangle$ at other temperatures calculated with our data are shown in Fig. 5. Also shown in the figure are the results obtained by NMR (Ref. 20) and diamagnetic anisotropy.²¹ Our results agree very well with previously reported values. Thus, the optical third-harmonic-generation method provides a correct determination of the order parameter $\langle P_2 \rangle$. This also strongly supports the reliability of the value of the order parameter $\langle P_4 \rangle$ determined within the same framework of analysis using the same set of data.

The parameters K_2 and K_4 in Eqs. (13) and (14), in general, depend on many components of the dressed molecular susceptibility γ_{ijkl}^* . As discussed in Sec. II, the component along the molecule long axis γ_{zzzz} usually

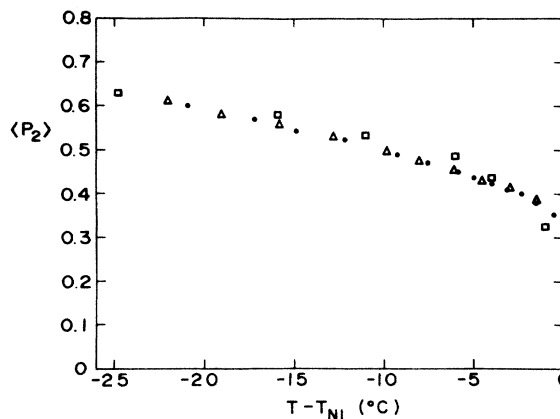


FIG. 5. $\langle P_2 \rangle$ of MBBA as function of temperature. ●, from third-harmonic-generation measurement; □, from NMR measurement (Ref. 20); △, from diamagnetic anisotropy measurement (Ref. 21).

dominates due to the extended delocalization of π electrons along the conjugated backbone. However, due to the difference in the contribution of the local-field correction along the molecular z and x axis (much larger along the x axis),¹² considerable enhancement would result in the dressed susceptibility γ_{xxxx}^* . It is thus reasonable to retain only γ_{zzz}^* and γ_{xxxx}^* in Eqs. (A4)–(A6). With the number of variables very much reduced, we can calculate K_4 from the value of $K_2=14.7$ obtained above. We get $\gamma_{xxxx}^*=0.22 \gamma_{zzz}^*$ and $K_4=1.78$. As discussed in Sec. II, the dominance of γ_{zzz}^* over the other components restricts the value of K_4 to be close to 2. Thus the choice of the value for γ_{xxxx}^* does not considerably affect our result for $\langle P_4 \rangle$. Using this value of K_4 , we obtain the value of $\langle P_4 \rangle$ for various temperatures as shown in Fig. 6. Also shown in the figure are the reported values for $\langle P_4 \rangle$ in neat MBBA from the Raman scattering method.² Within experimental error, the two results agree fairly well.

The third-harmonic-generation results allow consideration of whether or not the local-field tensor depends on the long-range anisotropy of the bulk medium as previously proposed in two-photon dichroism studies of the nematic phase.³ A tensor M is defined which describes the dependence of the local-field factor on the anisotropy of the bulk phase and is diagonalized in the laboratory coordinates along the axes parallel and perpendicular to the director. Then Eq. (12) can be rewritten as

$$\chi_{zzz}^{(3)} = (\delta + 2\xi \langle P_2 \rangle + 8\eta \langle P_4 \rangle) M_{\parallel}^4, \quad (20a)$$

$$\chi_{xxxx}^{(3)} = (\delta - \xi \langle P_2 \rangle + 3\eta \langle P_4 \rangle) M_{\perp}^4, \quad (20b)$$

$$\chi_{\text{iso}}^{(3)} = \delta M_{\text{iso}}^4, \quad (20c)$$

where M_{\parallel} and M_{\perp} are the eigenvalues of the diagonal matrix parallel and perpendicular to the nematic director. We introduce a corresponding quantity M_{iso} for the isotropic phase, with M_{iso} given by

$$M_{\text{iso}} = (M_{\parallel} + 2M_{\perp})/3. \quad (21)$$

Equation (13) is then rewritten as

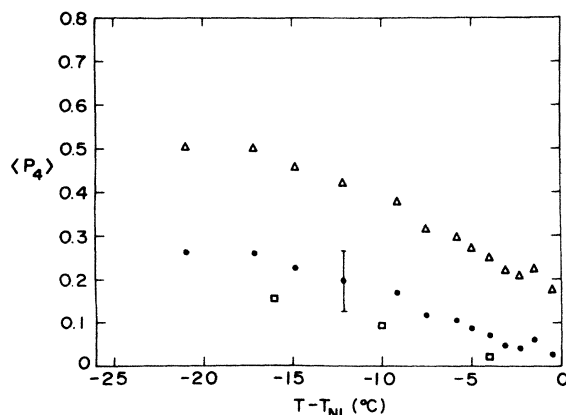


FIG. 6. $\langle P_4 \rangle$ of MBBA as function of temperature. ●, from third-harmonic-generation measurement with no long-range dependence of local field assumed; Δ, result from Eq. (22) with a long-range dependence of local field assumed; □, from Raman scattering measurement (Ref. 2).

$$\frac{\chi_{zzz}^{(3)}/M_{\parallel}^4 + 2\chi_{xxxx}^{(3)}/M_{\perp}^4}{\chi_{\text{iso}}^{(3)}/M_{\text{iso}}^4} = 3 + K_4 \langle P_4 \rangle. \quad (22)$$

Using the value of $M_{\perp}/M_{\parallel}=1.075$ previously assumed,³ the order parameter $\langle P_4 \rangle$ can be calculated using Eq. (22). The result is shown in Fig. 6. The resulting $\langle P_4 \rangle$ values are much larger than the values obtained from Raman scattering measurements² and from the present study where no long-range dependence of the local-field correction is assumed. Moreover, the $\langle P_4 \rangle$ values from Eq. (22) are much higher than values predicted by the Maier-Saupe mean-field theory. Thus, the experimental results from optical third-harmonic-generation measurements suggest that the local-field correction factor does not depend on the long-range anisotropy of the bulk medium. In the previous analysis,³ the molecule fixed local-field correction factor parallel and perpendicular to the molecule long axis is assumed to be the same. While it is apparent that the bare two-photon absorption tensor is dominated in effect by one principal component, the situation would be quite different in the dressed two-photon absorption tensor where the molecule fixed local fields are included. The present data show that the dressed susceptibility γ_{xxxx}^* is as much as 0.22 times that of γ_{zzz}^* , while we believe this number would be much smaller for the bare susceptibility. Thus, one can conclude that it is unlikely that the local-field correction tensor in the nematic phase depends on the long-range anisotropy of the bulk phase.

The role of the local-field correction factor in the nematic phase would be further elucidated if a comparison of the experimentally determined dressed susceptibility was made with a theoretically calculated bare susceptibility. This kind of investigation is in progress and will be the subject of future reports. Finally, we remark that the basis of this report could be extended to measurements of the fifth harmonic for the determination of the next higher-order parameter $\langle P_6 \rangle$. This, however, would be limited by the very weak response in fifth harmonic generation, and considerable resonance enhancement would be required.

In summary, we have developed a new method based on the measurement of optical third-harmonic generation for the determination of the orientational order parameters $\langle P_2 \rangle$ and $\langle P_4 \rangle$ of a nematic liquid crystal. The results obtained with this method are consistent with results reported based on NMR and Raman scattering measurements. Our results also show that it is unlikely that the local-field correction factor depends on the macroscopic anisotropy of the bulk.

ACKNOWLEDGMENTS

This research was funded by U.S. Air Force Office of Scientific Research (AFOSR) and U.S. Defense Advanced Projects Agency (DARPA), Contract No. F49620-85-C-0105 and National Science Foundation (Materials Research Laboratory Program) (NSF/MRL) Contract No. DMR-85-19059.

APPENDIX

Evaluation of the Macroscopic Susceptibility

The third-order susceptibility along the director axis of the bulk phase $\chi_{zzz}^{(3)}$ is given by Eq. (11)

$$\begin{aligned} \chi_{zzz}^{(3)} &= N \langle R_{zi} R_{zj} R_{zk} R_{zl} \gamma_{i'j'k'l'} \rangle \\ &= N \int_0^{2\pi} d\phi \int_0^\pi d\theta \sin\theta \int_0^{2\pi} d\psi F(\phi, \theta, \psi) \\ &\quad \times R_{zi} R_{zj} R_{zk} R_{zl} \gamma_{i'j'k'l'} , \end{aligned} \quad (\text{A1})$$

where $F(\phi, \theta, \psi)$ is the orientational distribution function at the Euler angles (ϕ, θ, ψ) . Here the microscopic susceptibility γ is understood to be the dressed susceptibility γ^* , we have dropped the asterisk for simplicity. The explicit form for the component of the rotation matrix $R(\phi, \theta, \psi)$ is given in Ref. 22. The nonvanishing contributions to $\chi_{zzz}^{(3)}$ are

$$\begin{aligned} \langle (R_{zz})^4 \gamma_{z'z'z'} \rangle &= \frac{\gamma_{z'z'z'}}{35} (7 + 20\langle P_2 \rangle + 8\langle P_4 \rangle) , \\ \langle (R_{xx})^4 \gamma_{x'x'x'} \rangle &= \frac{\gamma_{x'x'x'}}{35} (7 - 10\langle P_2 \rangle + 3\langle P_4 \rangle) , \\ \langle (R_{yy})^4 \gamma_{y'y'y'} \rangle &= \frac{\gamma_{y'y'y'}}{35} (7 - 10\langle P_2 \rangle + 3\langle P_4 \rangle) , \\ \langle (R_{zz})^2 (R_{zz})^2 \gamma_{z'z'x'} \rangle &= \frac{\gamma_{z'z'x'}}{105} (7 + 5\langle P_2 \rangle - 12\langle P_4 \rangle) , \\ \langle (R_{zz})^2 (R_{zz})^2 \gamma_{x'z'z'} \rangle &= \frac{\gamma_{x'z'z'}}{105} (7 + 5\langle P_2 \rangle - 12\langle P_4 \rangle) , \\ \langle (R_{zz})^2 (R_{yy})^2 \gamma_{z'z'y'} \rangle &= \frac{\gamma_{z'z'y'}}{105} (7 + 5\langle P_2 \rangle - 12\langle P_4 \rangle) , \\ \langle (R_{zz})^2 (R_{yy})^2 \gamma_{y'z'z'} \rangle &= \frac{\gamma_{y'z'z'}}{105} (7 + 5\langle P_2 \rangle - 12\langle P_4 \rangle) , \\ \langle (R_{zz})^2 (R_{yy})^2 \gamma_{x'x'y'} \rangle &= \frac{\gamma_{x'x'y'}}{105} (7 - 10\langle P_2 \rangle + 3\langle P_4 \rangle) , \\ \langle (R_{zz})^2 (R_{yy})^2 \gamma_{y'x'y'} \rangle &= \frac{\gamma_{y'x'y'}}{105} (7 - 10\langle P_2 \rangle + 3\langle P_4 \rangle) . \end{aligned}$$

Similarly the nonvanishing contributions to $\chi_{xxxx}^{(3)}$ are

$$\langle (R_{zz})^4 \gamma_{z'z'z'} \rangle = \frac{\gamma_{z'z'z'}}{35} (7 - 10\langle P_2 \rangle + 3\langle P_4 \rangle) ,$$

$$\langle (R_{xx})^4 \gamma_{x'x'x'} \rangle = \frac{\gamma_{x'x'x'}}{280} (56 + 40\langle P_2 \rangle + 9\langle P_4 \rangle) ,$$

$$\langle (R_{yy})^4 \gamma_{y'y'y'} \rangle = \frac{\gamma_{y'y'y'}}{280} (56 + 40\langle P_2 \rangle + 9\langle P_4 \rangle) ,$$

$$\langle (R_{zz})^2 (R_{xx})^2 \gamma_{z'z'x'} \rangle = \frac{\gamma_{z'z'x'}}{210} (14 - 5\langle P_2 \rangle - 9\langle P_4 \rangle) ,$$

$$\langle (R_{zz})^2 (R_{xx})^2 \gamma_{x'z'z'} \rangle = \frac{\gamma_{x'z'z'}}{210} (14 - 5\langle P_2 \rangle - 9\langle P_4 \rangle) ,$$

$$\langle (R_{zz})^2 (R_{yy})^2 \gamma_{z'z'y'} \rangle = \frac{\gamma_{z'z'y'}}{210} (14 - 5\langle P_2 \rangle - 9\langle P_4 \rangle) ,$$

$$\langle (R_{zz})^2 (R_{yy})^2 \gamma_{y'z'z'} \rangle = \frac{\gamma_{y'z'z'}}{210} (14 - 5\langle P_2 \rangle - 9\langle P_4 \rangle) ,$$

$$\langle (R_{xx})^2 (R_{yy})^2 \gamma_{x'x'y'} \rangle = \frac{\gamma_{x'x'y'}}{840} (56 + 40\langle P_2 \rangle + 9\langle P_4 \rangle) ,$$

$$\langle (R_{xx})^2 (R_{yy})^2 \gamma_{y'x'y'} \rangle = \frac{\gamma_{y'x'y'}}{840} (56 + 40\langle P_2 \rangle + 9\langle P_4 \rangle) .$$

We obtain

$$\chi_{zzz}^{(3)} = N (\delta + 2\xi\langle P_2 \rangle + 8\eta\langle P_4 \rangle) , \quad (\text{A2})$$

$$\chi_{xxxx}^{(3)} = N (\delta - \xi\langle P_2 \rangle + 3\eta\langle P_4 \rangle) , \quad (\text{A3})$$

where

$$\begin{aligned} \delta &= \frac{1}{5} (\gamma_{z'z'z'} + \gamma_{x'x'x'} + \gamma_{y'y'y'} + \gamma_{z'z'x'} \\ &\quad + \gamma_{x'z'z'} + \gamma_{z'z'y'} + \gamma_{y'z'z'} + \gamma_{x'x'y'} \\ &\quad + \gamma_{y'x'y'}) , \end{aligned} \quad (\text{A4})$$

$$\begin{aligned} \xi &= \frac{1}{14} (4\gamma_{z'z'z'} - 2\gamma_{x'x'x'} - 2\gamma_{y'y'y'} + \gamma_{z'z'x'} \\ &\quad + \gamma_{x'z'z'} + \gamma_{z'z'y'} + \gamma_{y'z'z'} - 2\gamma_{x'x'y'} \\ &\quad - 2\gamma_{y'x'y'}) , \end{aligned} \quad (\text{A5})$$

$$\begin{aligned} \eta &= \frac{1}{280} (8\gamma_{z'z'z'} + 3\gamma_{x'x'x'} + 3\gamma_{y'y'y'} - 12\gamma_{z'z'x'} \\ &\quad - 12\gamma_{x'z'z'} - 12\gamma_{z'z'y'} - 12\gamma_{y'z'z'} + 3\gamma_{x'x'y'} \\ &\quad + 3\gamma_{y'x'y'}) . \end{aligned} \quad (\text{A6})$$

In the isotropic phase, both $\langle P_2 \rangle$ and $\langle P_4 \rangle$ vanish. If we neglect the small variation of the particle density through the phase transition, we have

$$\chi_{\text{iso}}^{(3)} = N\delta . \quad (\text{A7})$$

¹For a general review see P. G. de Gennes, *The Physics of Liquid Crystals* (Clarendon, Oxford, 1974).

²S. Jen, N. A. Clark, P. S. Pershan, and E. B. Priestley, *J. Chem. Phys.* **66**, 4635 (1977).

³S. D. Durbin and Y. R. Shen, *Phys. Rev. A* **30**, 1419 (1984).

⁴S. K. Saha and G. K. Wong, *Appl. Phys. Lett.* **34**, 423 (1979).

⁵*Nonlinear Optical Properties of Organic and Polymeric Materials*, edited by D. Williams (Plenum, New York, 1983).

⁶A. F. Garito, C. C. Teng, K. Y. Wong, and O. Zamani-

Khamiri, *Mol. Cryst. Liq. Cryst.* **106B**, 219 (1984).

⁷A. Buka and W. H. de Jeu, *J. Phys.* **43**, 361 (1982).

⁸P. L. Sherrell and D. A. Crellin, *J. Phys. (Paris), Colloq.* **40**, C3-211 (1979).

⁹P. P. Karat and N. V. Madhusudana, *Mol. Cryst. Liq. Cryst.* **36**, 51 (1976).

¹⁰S. J. Lalama and A. F. Garito, *Phys. Rev. A* **20**, 1179 (1979).

¹¹A. N. Kuznetsov, V. A. Livshits, and S. G. Cheskis, *Sov. Phys. Crystallogr.* **20**, 142 (1975).

- ¹²W. H. de Jeu and P. Bordewijk, *J. Chem. Phys.* **68**, 109 (1978).
- ¹³J. Jerphagnon and S. K. Kurtz, *J. Appl. Phys.* **41**, 1667 (1970).
- ¹⁴W. H. de Jeu, *Physical Properties of Liquid Crystalline Materials* (Gordon and Breach, New York, 1980).
- ¹⁵S. Jen, N. A. Clark, P. S. Pershan, and E. B. Priestley, *Phys. Rev. Lett.* **31**, 1552 (1973).
- ¹⁶J. F. Ward and G. H. C. New, *Phys. Rev.* **185**, 57 (1969).
- ¹⁷G. R. Meredith, *Phys. Rev. B* **24**, 522 (1981).
- ¹⁸B. Buchalter and G. R. Meredith, *Appl. Opt.* **21**, 3221 (1982).
- ¹⁹S. Chandrasekhar and N. V. Madhusudana, *J. Phys. (Paris), Colloq.* **30**, C4-24 (1969).
- ²⁰Y. S. Lee, Y. Y. Hsu, and D. H. Dolphin, presentation at the ACS Symposium on Ordered Fluids and Liquid Crystals, Chicago, 1973 (unpublished).
- ²¹P. I. Rose, presentation at the Fourth International Conference on Liquid Crystals, Kent, Ohio, 1972 (unpublished).
- ²²M. E. Rose, *Elementary Theory of Angular Momentum* (Wiley, New York, 1957).